Multiparameter polarization-phase microscopy of optically anisotropic networks of biological crystals

Anatoly T. Stashkevich*[a], Natalia R. Kozan[b], Igor Yu. Oliynik[c], Lilia V.Hulei[c], Vitaliy P. Polevoy[c], Yuriy M. Solovey[c], Yuriy O. Ushenko[d], Olexander V. Dubolazov[d], Victor G. Paliy[e], Waldemar Wojcik[f], Gali Duskazaev[g], Ulzhalgas Zhunissova[h], Daniyar Jarykbassov[g]
[a]SI "The Institute of Traumatology and Orthopedics by NAMS of Ukraine, Bulvarno-Kudriavska St, 27, 01601 Kyiv, Ukraina; [b]Ivano-Frankivsk National Medical University Ministry of Public Health of Ukraine, Galytska 2, 76000 Ivano-Frankivsk, Ivano-Frankivsk, Ukraine; [c]Bukovinian State Medical University, 3 Theatral Sq., Chernivtsi, Ukraine, 58000; [d]Chernivtsi National University, 2 Kotsiubynskyi Str., Chernivtsi, Ukraine, 58012; [e]Vinnytsia National Pirogov Memorial Medical University, Pyrohova St, 56, Vinnytsia 21018, Ukraine; [f]Lublin University of Technology, Nadbystrzycka 38D, 20-618 Lublin, Poland; [g]Kazakh Academy of Transport and Communication, Almaty, Kazakhstan; [h]Astana Medical University, Nur-Sultan, Kazachstan

ABSTRACT

A new digital technique for objective differential diagnosis of the septic process severity was developed and experimentally tested by phase mapping of microscopic images of histological sections of polycrystalline internal organs and blood films of laboratory rats. the results of statistical analysis of histological sections of the internal organs of rats from control group 1 and research groups 2 to 4 with different severity of septic pathology are presented.

Keywords: polarization, Jones matrix, biological crystals, diagnostics

1. INTRODUCTION

Representative variances of the samples of histological sections of the internal organs of the following groups of rats are formed:

1) Intact rats - "control" group 1 (39 samples)
2) Sick rats (sepsis - light form) - "research" group 2:
    a. duration 12 hours. (39 samples) - “research” subgroup 2.1;
    b. duration 48 hours. (39 samples) - "research" subgroup 2.2.
3) Sick rats (sepsis - middle form) - "research" group 3:
    a. duration 12 hours. (39 samples) - “research” subgroup 3.1;
    b. duration 48 hours. (39 samples) - "research" subgroup 3.2..

2. METHOD FOR MEASURING COORDINATE DISTRIBUTIONS OF PHASE SHIFTS BETWEEN ORTHOGONAL COMPONENTS OF THE AMPLITUDE OF THE LASER RADIATION FIELD

This method is based on the formalism of the Jones matrix, the measurement scheme of which is classical and is presented in detail in works of 1. Wang[1], Tuchin[2], or Yao[3]:

$$U = \{P\}\{D\}\{A\}U_0 \quad (1)$$

were $\{P\}$ - polarizer Jones matrix; $\{D\}$ - Jones matrix of an optically uniaxial birefringent biological crystal; $\{A\}$ - analyzer Jones matrix; U_0 - Jones vector of the incident laser wave; U - Jones vector converted laser wave [1-5].

*e-mail: stashkat@i.ua

Photonics Applications in Astronomy, Communications, Industry, and High Energy Physics Experiments 2021
edited by Ryszard S. Romaniuk, Andrzej Smolarz, Waldemar Wojcik, Proc. of SPIE
Vol. 12040, 120400F · © 2021 SPIE · 0277-786X · doi: 10.1117/12.2617359

To directly experimentally determine the coordinate distribution of phase shifts $\delta(x,y)$ between the orthogonal amplitude components at the points $r \leftrightarrow (x,y)$ of the laser image of the optically anisotropic layer [6], it was proposed [6, 7] to place its sample between two crossed polarizing filters — quarter-wave plates and polarizers, the transmission planes of which are angles with axes of maximum speed +450 and - 450.

The amplitude E of the converted laser beam in such an experimental arrangement is determined by the equation

$$E = 0.25\{A\}\{\Phi_2\}\{\mathrm{M}\}\{\Phi_1\}\{P\}E_0 = 0.25\begin{Vmatrix} 1 & -1 \\ -1 & 1 \end{Vmatrix}\begin{Vmatrix} i & 0 \\ 0 & 1 \end{Vmatrix}\times$$
$$\times\begin{Vmatrix} \cos^2\rho+\sin^2\rho\exp[-i\delta] & \cos\rho\sin\rho\{1-\exp[-i\delta]\} \\ \cos\rho\sin\rho\{1-\exp[-i\delta]\} & \sin^2\rho+\cos^2\rho\exp[-i\delta] \end{Vmatrix}\times\begin{Vmatrix} 1 & 0 \\ 0 & i \end{Vmatrix}\begin{Vmatrix} 1 & 1 \\ 1 & 1 \end{Vmatrix}\begin{pmatrix} 1 \\ 1 \end{pmatrix}. \quad (2)$$

here {Φ1}, {Φ2} denote Jones matrices of quarter-wave plates.

The solution to the matrix equation (2) is the intensity $I(\delta)$ value at the point with the coordinates (x,y) of the laser image of the biological crystal [4,9,10].

$$I(\delta) = EE^{\otimes} = I_0\sin^2\left[\delta/2\right]. \quad (3)$$

An experimental measurement of the coordinate distributions of the magnitude of the phase shifts was carried out at the location of the laser micro-polarimeter, the optical scheme of which is given in scientific papers [10] and is presented in our work in Fig. 1.

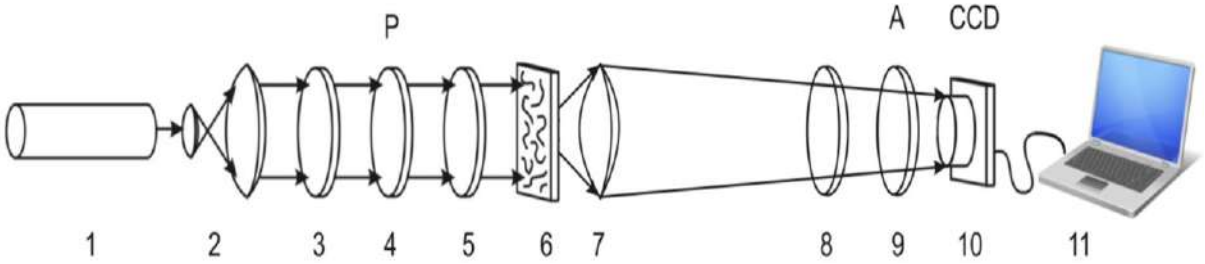

Figure 1. Optical design of a micro-polarimeter. Here: 1 - He-Ne laser; 2 - collimator; 3, 5, 8 - quarter-wave plates; 4, 9 - polarizer and analyzer, respectively; 6 - object of study; 7 - microlens.

The irradiation was carried out by a parallel beam (Ø = 10^4 μm) of a He-Ne laser (λ = 0.6328 μm) 1. A circularly polarized right beam was formed using a polarizing illuminator (quarter-wave plates 3, 5, and polarizer 4). The image of layers of biological tissues or fluids 6 was projected using a microlens 7 into the plane of the photosensitive area (800×600) of the CCD camera 10.

By rotating the transmitting axis of the analyzer 9 by an angle $\Theta = -45^0$ relative to the axis of the maximum speed of the quarter-wave plate 8, the conditions for transmitting left-circularly polarized oscillations of the laser image $I_\delta(m\times n)$ points for each individual pixel (mn) of the CCD camera were formed.

Then, according to relation (3), the coordinate distributions (phase maps) of phase shifts $\delta(m\times n)$ between the orthogonal components of the laser radiation amplitude of the image of the biological object were calculated [9,10,11].

3. DIFFERENTIAL DIAGNOSIS OF SEPSIS SEVERITY ACCORDING TO PHASE MAPS OF IMAGES OF HISTOLOGICAL SECTIONS OF THE SPLEEN

In a series of fragments of fig. 2 - fig. 3 shows phase maps (left column) of microscopic images of histological sections of the spleen and histograms of the distribution of phase shifts (right column) determined for biological preparations of rats from group 1 (fig. 2, (top row)), group 2.1 (fig. 2, (bottom row)), groups 3.1 (fig. 3, (top row)) and groups 4.1 (fig. 3, (bottom row)).

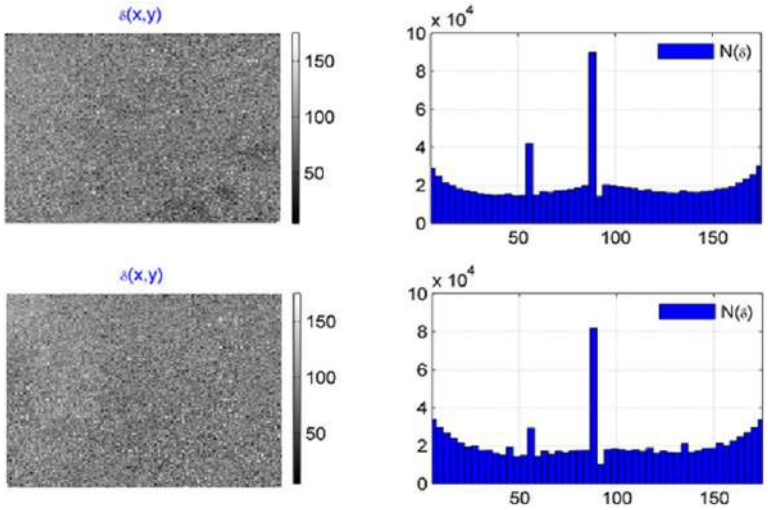

Figure 2. Phase maps and histograms of the distributions of the magnitude of phase shifts at the points of microscopic images of histological sections of the spleen of rats from group 1 and group 2.1.

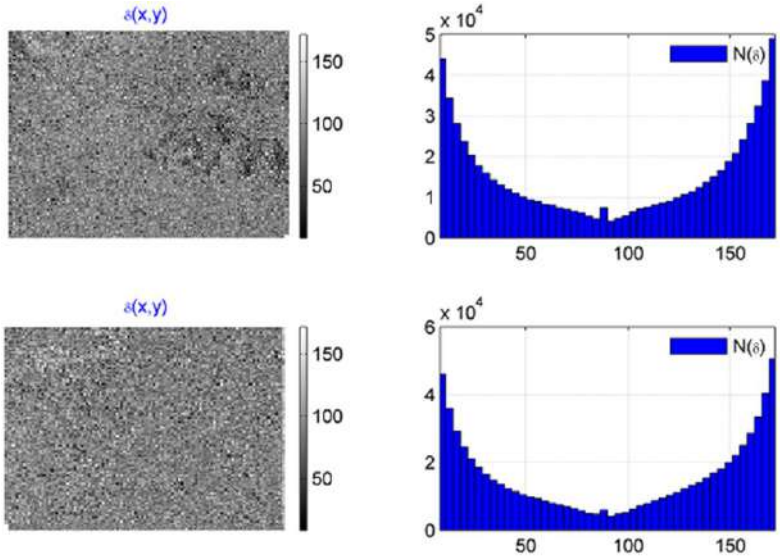

Figure 3. Phase maps and histograms of the distributions of the magnitude of phase shifts at the points of microscopic images of histological sections of the spleen of rats from group 3.1 and group 4.1.

A comparative analysis of the results of polarizing microscopic phasometry of microscopic images of the polycrystalline component of histological sections of the spleen has found:

- the presence of phase shift distributions, which are formed by the optical anisotropy mechanisms of the polycrystalline component of samples from all groups;
- the dependence of the statistical distributions of the magnitude of the phase shifts (right columns) at the points of digital microscopic images of histological sections of the spleen on the state of rats - healthy and septic affected;
- the difference for the intact and research groups of rats of the topographic and statistical structure of phase maps (left columns) of polarized-filtered digital microscopic images of biological preparations;
- the dependence on the severity of the septic process of the position of the main extreme of the histograms and the range of variation in the magnitude of the phases in the polarized filtered microscopic images (right columns in fig. 2 and fig. 3, respectively).

The quantitatively detected transformations of phase maps are illustrated by the statistical analysis data shown in table 1.

Table 1. Statistical parameters of phase maps of microscopic images of histological sections of the spleen [12].

Groups	**Group 1 Intact** $(n=39)$	**Group 2 Sepsis (light)** $(n=39)$		**Group 3 Sepsis (middle)** $(n=39)$		**Group 4 Sepsis (severe)** $(n=39)$	
Duration	**0 h.**	**2.1 (12 h.)**	**2.2 (48 h.)**	**3.1 (12 h.)**	**3.2 (48 h.)**	**4.1 (12 h.)**	**4.2 (48 h.)**
Average,*S*	1,23 ±0,059	1,02 ±0,044	0,85 ±0,038	0,72 ±0,033	0,56 ±0,021	0,43 ±0,027	0,36 ±0,022
Dispersion, *D*	1,04 ±0,043	0,89 ±0,041	0,66 ±0,028	0,48 ±0,021	0,34 ±0,014	0,26 ±0,015	0,21 ±0,014
Asymmetry,*A*	0,78 ±0,035	0,99 ±0,051	1,28 ±0,059	1,53 ±0,067	1,81 ±0,082	2,03 ±0,12	2,11 ±0,13
Excess, *E*	1,78 ±0,077	1,45 ±0,068	1,21 ±0,055	0,99 ±0,041	0,72 ±0,033	0,62 ±0,036	0,55 ±0,031

A comparative analysis of the values of the set of statistical moments of the 1st - 4th orders that characterize the histograms of the phase distributions at the points of microscopic images of histological sections of the spleen revealed:

1) Central statistical moment of the 1st order (average S):
   a. the average group S value within the range of representative samples "group 1 - group 4" decreases from 1.23 to 0.36;
   b. intergroup differences - statistically significant ($p_{1\div4}, p_{2\div3}, p_{3\div4}, p_{2\div4} \prec$);
2) The central statistical moment of the 2nd order (dispersion D):
   a. the average group dispersion within the set of representative samples “group 1 - group 4” decreases from 1.04 to 0.31;
   b. intergroup differences - statistically significant for all groups ($p_{1\div4}, p_{2\div3}, p_{3\div4}, p_{2\div4} \prec$);
3) The central statistical moment of the 3rd order (asymmetry A):
   a. the average group value of asymmetry A within the aggregate of representative samples “group 1 - group 4” grows in the range from 0.78 to 2.11;
   b. intergroup differences - statistically significant for all groups ($p_{1\div4}, p_{2\div3}, p_{3\div4}, p_{2\div4} \prec$)
4) The central statistical moment of the 4th order (excess E):
   a. the group average excess E within the range of representative samples “group 1 - group 4” decreases from 1.78 to 0.55;
5) intergroup differences - statistically significant ($p_{1\div4}, p_{2\div3}, p_{3\div4}, p_{2\div4} \prec$).
6) For all statistical moments, the intergroup differences "4.1-4.2" are statistically unreliable $p_{4.1-4.2} \succ$.

4. OPERATIONAL CHARACTERISTICS OF THE STRENGTH OF THE METHOD OF DIFFERENTIAL DIAGNOSIS OF SEPSIS SEVERITY ACCORDING TO PHASE MAPS OF IMAGES OF HISTOLOGICAL SECTIONS OF THE SPLEEN

When conducting an information analysis of the data of the polarization-phase microscopy method, we will use the terminology – “operational characteristics of the diagnostic force” [13 - 18]:

- Interpretation "positive" for rats with the presence of the disease - "truly positive case" – ($TP \equiv a$).
- Interpretation "negative" for rats with no disease - "true negative case"– ($TN \equiv c$).
- Interpretation "positive" for rats with no disease - "false positive case" – ($FP \equiv b$).
- Interpretation "negative" for rats with the presence of the disease - "false negative case"– ($FN \equiv d$).

The following group of operational characteristics is applied. Sensitivity (Se) i.e. the proportion of correct positive results (TP) of the phasemetry of biological preparations of all sick rats (D_+) $Se = TP/D_+ \cdot 100\%$. Specificity (Sp) – this is the proportion of correct negative results TN of the phasemetry method of biological preparations among a group of healthy rats ($D\_$) $Sp = TN/D\_ \cdot 100\%$. Accuracy (Ac) – proportion of correct results ($TP+TN$) of the phase preparation test of biological preparations among all the studied rats ($D_+ + D\_$) $Ac = \frac{TP+TN}{D_+ + D\_} 100\%$.

Table 3. Information on video and audio files that can accompany a manuscript submission.

Groups	"1 – (2,3,4)"	"2-3"	"2-4"	"3-4"
Average,*S*	$\left\{\begin{matrix} a=31;b=8; \\ c=30;d=9 \end{matrix}\right\}$ **78,2**	$\left\{\begin{matrix} a=31;b=8; \\ c=29;d=10 \end{matrix}\right\}$ **76,9**	$\left\{\begin{matrix} a=31;b=8; \\ c=30;d=9 \end{matrix}\right\}$ **78,2**	$\left\{\begin{matrix} a=31;b=8; \\ c=30;d=9 \end{matrix}\right\}$ **78,2**
Dispersion, *D*	$\left\{\begin{matrix} a=31;b=8; \\ c=31;d=8 \end{matrix}\right\}$ **79,5**	$\left\{\begin{matrix} a=30;b=9; \\ c=30;d=9 \end{matrix}\right\}$ **76,9**	$\left\{\begin{matrix} a=31;b=8; \\ c=30;d=9 \end{matrix}\right\}$ **78,2**	$\left\{\begin{matrix} a=31;b=8; \\ c=30;d=9 \end{matrix}\right\}$ **78,2**
Asymmetry,*A*	$\left\{\begin{matrix} a=37;b=2; \\ c=37;d=2 \end{matrix}\right\}$ **94,8**	$\left\{\begin{matrix} a=37;b=2; \\ c=35;d=4 \end{matrix}\right\}$ **92,3**	$\left\{\begin{matrix} a=37;b=2; \\ c=36;d=3 \end{matrix}\right\}$ **93.6**	$\left\{\begin{matrix} a=33;b=6; \\ c=33;d=6 \end{matrix}\right\}$ **84,6**
Excess, *E*	$\left\{\begin{matrix} a=35;b=4; \\ c=36;d=3 \end{matrix}\right\}$ **91**	$\left\{\begin{matrix} a=36;b=3; \\ c=35;d=4 \end{matrix}\right\}$ **91**	$\left\{\begin{matrix} a=37;b=1; \\ c=36;d=3 \end{matrix}\right\}$ **94,8**	$\left\{\begin{matrix} a=31;b=8; \\ c=30;d=9 \end{matrix}\right\}$ **78,2**

Groups	"2.1 – 2.2"	"3.1-3.2"	"4.1-4.2"
Average,*S*	$\left\{\begin{matrix} a=32;b=7; \\ c=32;d=7 \end{matrix}\right\}$ **82,1**	$\left\{\begin{matrix} a=30;b=9; \\ c=29;d=10 \end{matrix}\right\}$ **75,6**	$\left\{\begin{matrix} a=22;b=17; \\ c=20;d=19 \end{matrix}\right\}$ **53,2**
Dispersion, *D*	$\left\{\begin{matrix} a=30;b=9; \\ c=29;d=10 \end{matrix}\right\}$ **75,6**	$\left\{\begin{matrix} a=28;b=11; \\ c=28;d=11 \end{matrix}\right\}$ **70,5**	$\left\{\begin{matrix} a=22;b=17; \\ c=22;d=17 \end{matrix}\right\}$ **55,4**
Asymmetry,*A*	$\left\{\begin{matrix} a=36;b=3; \\ c=36;d=3 \end{matrix}\right\}$ **92,3**	$\left\{\begin{matrix} a=35;b=4; \\ c=34;d=5 \end{matrix}\right\}$ **88,5**	$\left\{\begin{matrix} a=24;b=15; \\ c=23;d=16 \end{matrix}\right\}$ **60,3**
Excess, *E*	$\left\{\begin{matrix} a=35;b=4; \\ c=34;d=5 \end{matrix}\right\}$ **88,5**	$\left\{\begin{matrix} a=34;b=5; \\ c=31;d=8 \end{matrix}\right\}$ **83,3**	$\left\{\begin{matrix} a=22;b=17; \\ c=22;d=17 \end{matrix}\right\}$ **55,4**

The following ranges of maximum balanced accuracy were identified:

- intact - patients "1 - (2,3,4)" - excellent quality $Ac(A.E)=91\%-94{,}8\%$;
- light - medium grade "2-3" - excellent quality $Ac(A.E)=91\%-92{,}3\%$;
- light - severe degree "2-4" - excellent quality $Ac(A)=92{,}3\%$;
- medium - severe degree "3-4" - good quality $Ac(A)=84{,}6\%$;
- internal group light degree "2.1 - 2.2" - excellent quality $Ac(A.E)=91\%-93{,}6\%$;
- the internal group average degree "3.1 - 3.2" - very good quality $Ac(A)=88{,}5\%$;
- the internal group severe degree "4.1 - 4.2" - unsatisfactory quality $Ac \prec 70\%$.

CONCLUSIONS

The optical arrangement of the system of phasometric mapping of microscopic images of histological sections of the internal organs of laboratory rats was experimentally tested. An album of maps of the distribution of the magnitude of the phase points of a digital microscopic image of histological sections of internal organs and blood films from control group 1 and research groups 2–4 with different severity of septic pathology was obtained. The most diagnostic-sensitive

statistical criteria for the differentiation of phase maps of microscopic images of histological sections of the internal organs of rats from control group 1 and research groups 2 - 4 with different septic pathology severity were found. The operational characteristics of the diagnostic strength of the method of polarization-phase microscopy of histological sections of tissues of the internal organs of the control and experimental groups are determined. Established balanced accuracy:

- - differentiation of healthy and septic rats;
- - intergroup differentiation of septic process severity in sick rats;
- - intra-group differentiation of septic patients in rats.

REFERENCES

[1] Wang, X. and Wang, L.-H., "Propagation of polarized light in birefringent turbid media: a Monte Carlo study," J. Biomed. Opt. Vol. 7, 279-290 (2002).

[2] Tuchin, V. V., [Handbook of optical biomedical diagnostics], SPIE Press, Bellingham, 1–1110, (2002).

[3] Yao G. and Wang L. V., "Two-dimensional depth-resolved Mueller matrix characterization of biological tissue by optical coherence tomography," Opt. Lett., Vol. 24., 537-539 (1999).

[4] Tower, T. T. and Tranquillo, R. T. "Alignment Maps of Tissues: I. Microscopic Elliptical Polarimetry," Biophys. J., Vol. 81, 2954-2963 (2001).

[5] Lu, S. and Chipman R. A., "Interpretation of Mueller matrices based on polar decomposition," J. Opt. Soc. Am. A., Vol. 13, 1106-1113 (1996).

[6] Ghosh, N. and Vitkin, I. A., "Techniques for fast and sensitive measurements of two-dimensional birefringence distributions," Journal of Biomedical Optics., 16(11), 110801 (2011).

[7] Tuchin, V. V., Wang, L. and Zimnyakov, D. A., [Optical polarization in biomedical applications], New York, USA (2006).

[8] Ushenko, A.G., Dubolazov, O.V., Bachynsky, V.T., Peresunko, A.P. and Vanchulyak, O.Y., "On the feasibilities of using the wavelet analysis of mueller matrix images of biological crystals," Advances in Optical Technologies, 162832 (2010)

[9] Zabolotna, N.I., Wojcik, W., Pavlov, S.V., Ushenko, O.G. and Suleimenov, B., "Diagnostics of pathologically changed birefringent networks by means of phase Mueller matrix tomography," Proceedings of SPIE 86980E (2013).

[10] Ushenko, A.G., "Correlation Processing and wavelet analysis of polarization images of biological tissues," Optics and Spectroscopy (OptikaiSpektroskopiya), 91 (5), 773-778 (2001).

[11] Isaieva, O. A., Avrunin, O. G., Moroz, I. I., Stoliarenko, O. V., Akselrod, R. B., Kylyvnyk, V. S., and Kozbakova, A., "Features of image analysis under UV-video dermoscopy," Proceedings of SPIE - the International Society for Optical Engineering, 11456 (2020).

[12] Kovalova, A., Shushliapina, N., Avrunin, O., Zlepko, A., Pugach, S., Burennikova, N. and Smailova, S., "Possibilities of automated image processing at optical capillaroscopy," Proceedings of SPIE - the International Society for Optical Engineering, 11456 (2020).

[13] Selivanova, K. G., Avrunin, O. G., Zlepko, S., Guminskyi, Y. Y., Poplavskyy, O. A. and Gromaszek, K., "The tracking system of a three-dimensional position of hand movement fortremor detection," Proceedings of SPIE 115810I (2020).

[14] Waldemar, W., Smolarz, A. and Pavlov, S. V., [Information technology in medical diagnostics], Taylor & Francis Group, CRC Press, Balkema book, London, 1-210 (2017).

[15] Kozlovska, T. I., Kolisnik, P. F., Zlepko, S. M., et al., "Physical-mathematical model of optical radiation interaction with biological tissues," Proc. SPIE 10445, (2017).

[16] Omiotek, Z., Prokop, P., "The construction of the feature vector in the diagnosis of sarcoidosis based on the fractal analysis of CT chet images," Informatyka, Automatyka, Pomiary W Gospodarce I Ochronie Środowiska, 9(2), 16-23 (2019).

[17] Korchenko, A., Tereykovcky, I., Aytkhozhaeva, E., Seilova, N., Kosyuk, Y., Wojcik, W., Komada, P. & Sikora, J.,"Efficiency evaluating method for the devices with infrasound impact on the computer equipment functioning," International Journal of Electronics and Telecommunications, 64(2) (2018).

[18] Kozlovska, T. I. and Pavlov, S. V., [Optoelectronic means of diagnosing human pathologies associated with peripheral blood circulation] LAP LAMBERT Academic Publishing, Mauritius, 1–56 (2019).